Indian Journal of Chemistry
Vol. 64, November 2025, pp. 1059-1067
DOI: 10.56042/ijc.v64i11.19797

Microwave-assisted green synthesis of nickel nanoparticles using *Tinospora cordifolia* stem extract and its application as a photocatalyst

Sanjay Kumar Upadhyay, Vishant Varma & Devbrat Pundhir*
Nano Research Laboratory,
Department of Applied Sciences and Humanities (Chemistry),
Raja Balwant Singh Engineering Technical Campus, Bichpuri, Agra 283 105, India
Seismo-electromagnetics & Space Research Laboratory,
Department of Applied Sciences and Humanities (Physics),
Raja Balwant Singh Engineering Technical Campus, Bichpuri, Agra 283 105, India
E-mail: devbratpundhir@gmail.com, sanjay_upadh11j@rediffmail.com, vishantvarma786@gmail.com

Received 17 May 2025; accepted (revised) 6 October 2025

The synthesis of nanoparticles using environmental friendly methods has gained significant attention in recent years due to the growing concerns regarding the environmental impact of traditional synthetic techniques. Microwave-assisted green synthesis offers a promising solution by combining the advantages of microwave irradiation and green chemistry principles. The green approach utilizes eco-friendly precursors and reducing agents, such as plant extracts and natural polymers, to minimize the use of hazardous materials and reduces waste generation. In this study, nickel nanoparticles are formed using *Tinospora cordifolia*'s stem extract as a reducing agent and nickel nitrate hexahydrate as a reaction precursor. The UV-Vis analysis has confirmed their formation in the wavelength range between 200 nm and 800 nm, and the maximum wavelength is observed at 365 nm with an absorbance of 0.865. The SEM image confirms its topography with a large variation in the size, and its distribution varied in the range of 40-80 nm. Ni-NPs show 41.34% degradation of methylene blue and 28.9% of methyl orange. Low efficiency of photocatalytic activity has been observed due to higher concentration of dyes, shorter reaction time and lower concentration of plant mediated Nickel nanoparticles.

Keywords: Nanoparticles, Microwave, Green Synthesis, SEM

In recent years, metallic nanoparticles (NPs) have garnered considerable interest across scientific and industrial domains due to their unique physicochemical properties and wide-ranging applications[1]. A critical challenge in this field is the development of efficient, sustainable synthesis methods. While various techniques, including chemical and green synthesis, are employed[2], conventional chemical methods often involve hazardous reagents and generate substantial waste, posing environmental and health risks[3].

Researchers have increasingly adopted green synthesis approaches emphasizing sustainability and reducing ecological impact[4]. Among these, microwave-assisted green synthesis has emerged as a highly efficient method, offering rapid and uniform heating that accelerates reaction kinetics and enhances product yield[5,6]. This method aligns closely with the principles of green chemistry, which advocate for minimizing toxic inputs, reducing waste, and improving energy efficiency[7].

Microwave-assisted green synthesis typically employs environmentally benign reducing and stabilizing agents, such as plant extracts, biopolymers, and other renewable materials, to further reduce environmental impact[8]. One such agent is *Tinospora cordifolia*, a medicinal plant native to the Indian subcontinent and China, widely used in Ayurveda. It is of particular interest due to its rich composition of bioactive compounds, including steroids, phenolics, alkaloids, sesquiterpenoids, diterpenoids, aliphatic compounds, and polysaccharides[9,10].

The increasing demand for nanomaterials across sectors such as catalysis, energy storage, and environmental remediation underscores the need for sustainable synthesis methods[1]. Nickel nanoparticles (Ni-NPs), known for their excellent catalytic, magnetic, and electronic properties, are especially promising in this context[4-11].

Several studies have demonstrated the successful synthesis of Ni-NPs *via* microwave-assisted green

methods[2-12]. Reduced nickel acetate tetrahydrate under microwave irradiation, producing Ni-NPs with sizes ranging from 3.8 to 7.1 nm[13]. synthesized NiO-NPs using Clerodendrum phlomidis leaf extract and nickel nitrate, reporting a UV-Vis absorption peak at 329 nm and a particle size of 10.7 ± 1.3 nm with spherical morphology confirmed *via* HRTEM[14]. used Andrographis paniculata leaf extract for NiO-NP synthesis under microwave irradiation, yielding particles with an average size of 24 nm. The particles exhibited a band gap of 3.51 eV and photoluminescence peaks at 350, 439, 485, and 530 nm, along with demonstrated anticancer activity.

Microwave-assisted green synthesized nickel nanoparticles (Ni-NPs) attracted attention due to their ability to degrade organic dyes, which are persistent pollutants in wastewater[15]. The photocatalytic activity of Ni-NPs is based on the absorption of light. When Ni-NPs absorbed incident light, they generated electron-hole pairs. The excited electrons reacted with oxygen and water to generate reactive oxygen species, decomposing organic dyes into less harmful compounds[3]. The photocatalytic activity of nickel NPs is affected by the size, surface area, and morphology of nanoparticles, shape and functional groups of dyes, and reaction conditions (*e.g.*, time, temperature, light intensity, and *p*H). Several studies have investigated the degradation of organic dyes by synthesized nickel nanoparticles[16]. Microwave-assisted synthesis was chosen for our study due to its ability to control the nanoparticles' size and shape by varying parameters such as temperature, reaction time, pressure, and reactant concentration[17].

Keeping the above in view, nickel nitrate hexahydrate was used as a precursor, and *Tinospora cordifolia* stem extract acted as the reducing agent. The synthesized nickel nanoparticles were characterized using several techniques[6]. The ultraviolet-visible (UV-Vis) spectroscopy was used to confirm the topology of the nanoparticles, with a maximum absorption peak observed at 365 nm, indicating their successful formation. Scanning electron microscopy (SEM) was used to investigate the size and shape distribution of the nanoparticles, providing insights into their morphology[18]. Energy-dispersive X-ray spectroscopy (EDS) analysis further evaluated the purity and composition of the synthesized nanoparticles, confirming the presence of nickel and successful reduction by plant extracts. The photocatalytic activity of these particles has also been examined against organic dyes. The dyes are usually coloured because they absorb light in the visible spectrum (350-700 nm), contain at least one chromophore (such as nitro, azo, anthraquinone, phthalocyanine, and methyl group, *etc*.), and have a conjugated system. Apart from chromophore, most of the dyes contain colour-enhancing groups known as auxochromes, such as -COOH, -SO_3H, -OH, *etc*., groups which also affect the solubility of the dye. If any of these features are affected or leaked from the molecular structure, the colour of the dye is lost[19]. The catalytic performance of the synthesized Ni-NPs was observed using UV-Vis spectroscopy[20]. The molecular structure of methyl orange consists of an azo group that combines with a benzene ring and a sulfonic acid moiety to give the dye its orange colour. Methylene blue contains a phenothiazine core, a tricyclic structure consisting of a benzene ring fused to a thiazine ring. An imine (–C=N–) functional group contributes to its colour properties. The presence of a sulfonium group (–S+) increases its solubility in water[19].

Methods of Microwave-Assisted Green Synthesis

The microwave-assisted green synthesis method typically involves the following steps:-

Selection of green precursors and reducing agents

Eco-friendly materials are chosen as precursors and reducing agents based on availability, biocompatibility, and reducing potential[21]. *Tinospora cordifolia* stem extract has phytochemical constituents like alkaloids, carbohydrates, cardiac glycosides, flavonoids, proteins, resins, saponins, steroids, and tannins which are confirmed by tests such as Mayer's test, Benedict test, Borntrager's test, Alkaline reagent test, Ninhydrin test, lead acetate test, Ferric chloride test, respectively. Due to the presence of alkaloidal properties, the *T. cordifolia* stem is selected for the synthesis of nanoparticles of various metals because alkaloids work as the best reducing agent.

The details of tests for phytochemical properties present in *Tinospora cordifolia* extract include[22] the following.

(i) Alkaloids Detection (Mayer's test): Mayer's reagent is added to the extract, resulting in a creamy white precipitate if alkaloids are present.

(ii) Carbohydrates Detection (Benedict's test): Benedict's reagent, mixed with the extract and heated, results in a red precipitate, which indicates the presence of sugars.

(iii) **Cardiac Glycosides Detection (Borntrager's test**): Chloroform and Ammonia are mixed with the extract, followed by the appearance of a pink colour in the chloroform layer, indicating the presence of cardiac glycosides.

(iv) **Flavonoids Detection (Alkaline reagent test):** Aluminium chloride and concentrated Sulfuric Acid were added to the extract, resulting in a yellow colour if flavonoids are present.

(v) **Protein Detection (Ninhydrin test):** Ninhydrin reagent is added to the extract and heated, producing a purple colour if proteins are present.

(vi) **Resins Detection:** Ferric Chloride and potassium Ferricyanide were added to the extract and heated, producing a green or blue colour, if resins are present.

(vii) **Saponins Detection (Lead Acetate test):** Lead Acetate solution is mixed with the extract, resulting in the formation of white precipitates, if saponins are present.

(viii) **Steroids Detection:** Chloroform, Acetic anhydride, and concentrated Sulphuric acid were added to the extract, resulting in a blue-green colour, if steroids are present.

(ix) **Tannins Detection (Ferric chloride test):** Ferric Chloride solution is added to the extract which results, a violet or greenish colour, if tannins are present.

Preparation of Plant Extract

The stems of *T. cordifolia* were collected from the garden of the boys' hostel located in the premises of Raja Balwant Singh Engineering Technical Campus, Bichpuri Agra, India, and washed properly several times to remove dust and other environmentally polluting particles, and then cut into small pieces about 1-2 inches long, after cutting, dried in a hot air oven for 10 minutes and then soaked in air for 15 minutes. This cycle was repeated until the stems were completely dried. Dried stems were crushed and converted into fine powder with the help of a mixer /grinder. A 10g powder was dissolved in 100 mL of water and boiled for 30 minutes or until the solution was reduced to half of its initial volume. Finally, it was filtered with the help of Whatman no. 1 filter paper and stored at 4°C for further use[10].

Preparation of Reaction Mixture

Nickel nitrate hexahydrate (Merck) was selected as the reaction precursor for the synthesis of nickel nanoparticles, and 0.5M nickel salt solution was used for the synthesis. *T. cordifolia* stem powder extract is used as a reducing agent. A 20 mL of nickel salt solution and 30 mL of stem powder extract solution were mixed in a 100 mL conical flask, and further, it was subjected to microwave irradiation[1].

Microwave Irradiation and Synthesis

The reaction mixture is exposed to microwave irradiation, which rapidly heats the mixture and promotes the nucleation and growth of nanoparticles. A precise control over reaction parameters such as temperature and irradiation time allowed nanoparticle synthesis optimization. The mixture of salt solution and extract solution was kept in the microwave oven at 230°C for 30 minutes with 20 minutes of continued stirring. After 30 minutes, the colour of the mixture changed from green to dark green, which indicated the formation of nickel nanoparticles[23]. Further, the formation of Ni nanoparticles was confirmed by the different characterization techniques. A schematic overview of the formation of microwave-assisted Ni-nanoparticles is shown in Fig. 1.

Results and Discussion

The synthesized nanoparticles were characterized using different characterization techniques, such as SEM and UV-Vis spectrophotometer. In Fig. 2, UV-Vis spectrophotometer results show the formation and stability of synthesized nickel nanoparticles in the wavelength range between 200nm and 800nm. The first peak value of wavelength was observed at 365 nm, and the absorbance of 0.865 (Ref. 22-24). This indicates a high absorption in the near-UV region. A second, smaller peak is visible around 600 nm, with an absorbance of approximately 0.65 AU. A noticeable minimum (trough) in absorbance appears around 480-500 nm, where the absorbance drops to around 0.35 AU. After the second peak, the spectrum plateaus slightly above 0.6 AU from 700 to 900 nm, suggesting stable absorbance in the near-infrared region. The peaks in the UV-Vis spectrum typically correspond to electronic transitions, such as $\pi \rightarrow \pi^*$ or $n \rightarrow \pi^*$. The strong peak near 360 nm suggests a $\pi \rightarrow \pi^*$ transition, common in compounds with conjugated systems or aromatic rings. The presence of multiple absorbance peaks implies that the compound has a complex electronic structure. The peak at 365 nm is likely due to conjugated double bonds or aromatic groups. The shoulder or secondary peak in the visible range (600 nm) might be due to d-d

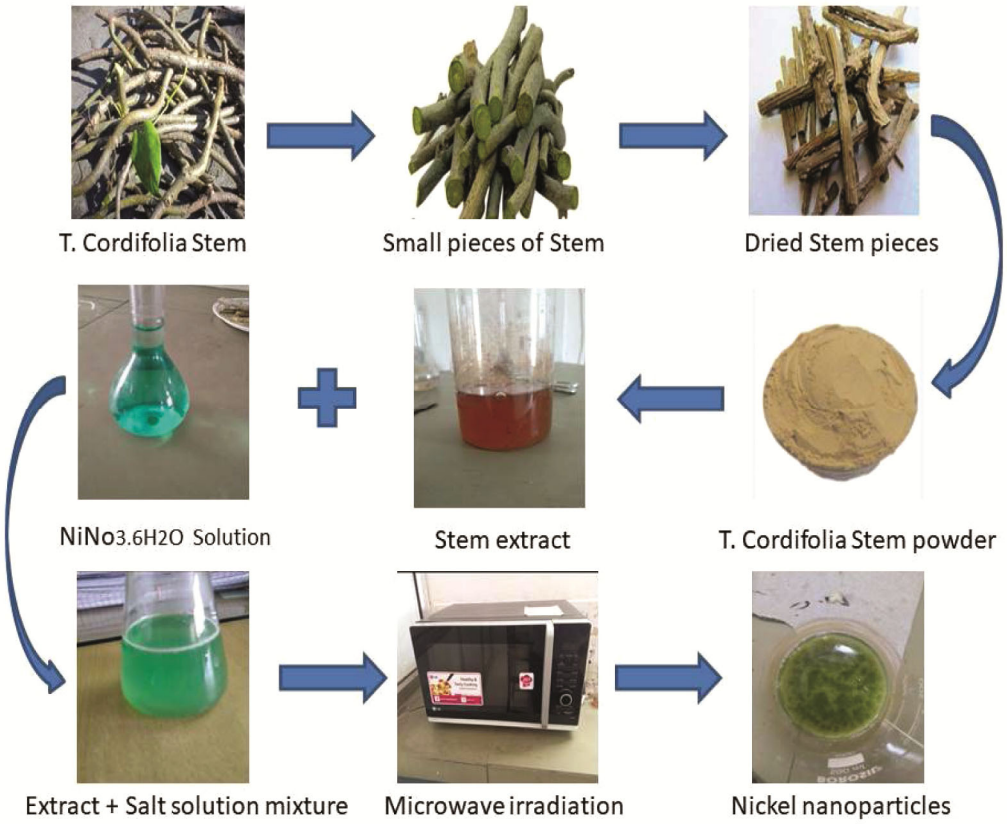

Fig. 1 — Schematic diagram of microwave-assisted green synthesis of nickel NPs

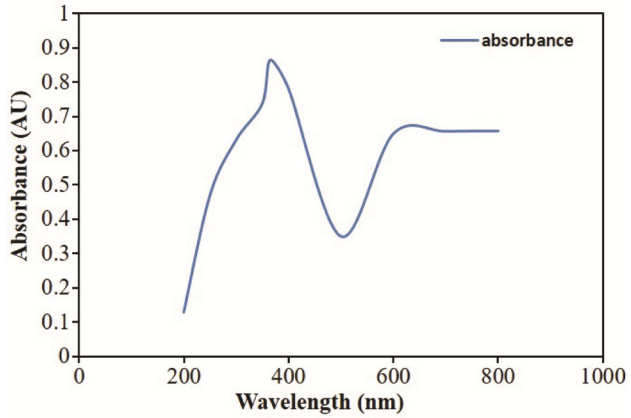

Fig. 2 — Results in the UV-Vis spectrophotometer of NiNPs

transitions (in the case of transition metal complexes) or charge transfer transitions. These results are very similar to the study of earlier workers[6].

A Scanning Electron Microscope (SEM) image of the synthesized Ni-nanoparticles was taken at a magnification of 110,000× (Fig. 3a), with an accelerating voltage of 15.0 kV using a JEOL SEM system. The scale bar indicates 100 nm, suggesting that the observed material is in the nanostructured range, likely composed of nanoparticles or nanoclusters, which indicates that sample grinding appears incomplete and large variation in the size of the particles[22]. The SEM images confirmed the formation of these nanoparticles and the large size distribution of the synthesized nickel nanoparticles by *T. cordifolia* stem extract. The particle size range of 40 to 80nm and the average particle size of 30nm have been observed, which is highlighted in the figure by a rectangle. It reveals that the sample surface is composed of aggregated nanoparticles, forming a highly porous and rough texture. The particles appear to be irregular in shape but are generally closely packed, creating a network-like structure. The particles tend to agglomerate due to high surface energy and Vanderwaal's forces. The nanoscale texture enhances surface reactivity, electron transport, and mass diffusion, making the material suitable for advanced functional applications. Additionally, the compact yet porous arrangement may allow for good accessibility of active sites if used in catalysis or adsorption. Suppose the SEM is part of a characterization set for a synthesized material (*e.g.*, metal oxide, polymer nanocomposite, *etc*.). In that

case, it strongly supports the successful formation of nanostructures with the desired morphology.

Another SEM image was taken at a magnification of 50,000× (Fig. 3b), using a 15.0 kV accelerating voltage, with a scale bar of 100 nm, using the previously used system. This micrograph provides a detailed view of the surface morphology of a nanostructured material, potentially used in fields such as catalysis, energy storage, or sensing applications. The surface appears to be composed of irregularly shaped closely packed nanoparticles with varying grain sizes. As compared to the previous image (at 110,000×), this image, at a lower magnification, gives a broader overview of the surface texture. The particles exhibit a rough, porous structure with distinct voids and cavities distributed throughout the material. The average size of particles is similar to the previous one, *i.e.*, size range of 40 to 80nm, and the average particle size of 30nm has been observed, which is highlighted in the figure by a rectangle. These features suggest the presence of interparticle porosity, which can enhance mass transport and surface accessibility. This kind of morphology indicates a material with a high surface area and potential mesoporous characteristics, which are advantageous for applications like adsorption, photocatalysis, or electrochemical energy storage. The dark spots or voids could be beneficial in facilitating ion diffusion or increasing active site exposure, depending on the functional purpose of the material. The aggregation of particles may be attributed to synthesis conditions (*e.g.*, sol-gel, hydrothermal, or co-precipitation techniques) that often lead to nanoparticle clustering due to surface energy minimization.

Overall, these images support the successful fabrication of a nanostructured material with a porous network, which could contribute to enhanced performance in its target application.

The EDS results of nanoparticles are shown in Fig. 4. It shows the chemical composition and purity of the synthesized nickel nanoparticles. It can be seen in EDS images of our samples that the nickel nanoparticles were present in the major composition, about 57.6%. Nickel nanoparticles show magnetic behaviour that was confirmed by the magnetic bar [4]. The colour of the solution disappeared, indicating the efficient performance of the catalyst. The absorbance of this mixture was determined by UV-Vis spectroscopy within specific intervals[25]. The sharp peaks indicate the presence of various elements in the analyzed region. Major elements detected include. Nickel (Ni) shows several distinct peaks, highest at around 0.85 keV and additional at higher energies. The weight percentage (Wt%) of Ni is the highest at 57.6%, indicating it is the primary component of the sample. Oxygen (O) has a prominent peak near 0.5 keV, with a substantial contribution of 38.1% Wt%, suggesting the presence of oxides or other oxygen-containing compounds. Nitrogen (N) exhibits a smaller peak at approximately 0.39 keV and constitutes 2.4% Wt%, possibly indicating nitrides or adsorbed nitrogen-containing species. Sulfur (S) and Chlorine (Cl) show minor peaks in the 2–3 keV region with 1.0% and 0.9% Wt% respectively, indicating trace amounts, possibly from surface contamination or specific compounds. Platinum (Pt) was detected through several peaks (*e.g.*, at ~2.05 keV and higher), likely indicating a coating material used in SEM sample preparation or a component of the sample itself. Despite clear peaks, no weight percentage is listed for Pt in the legend, which might

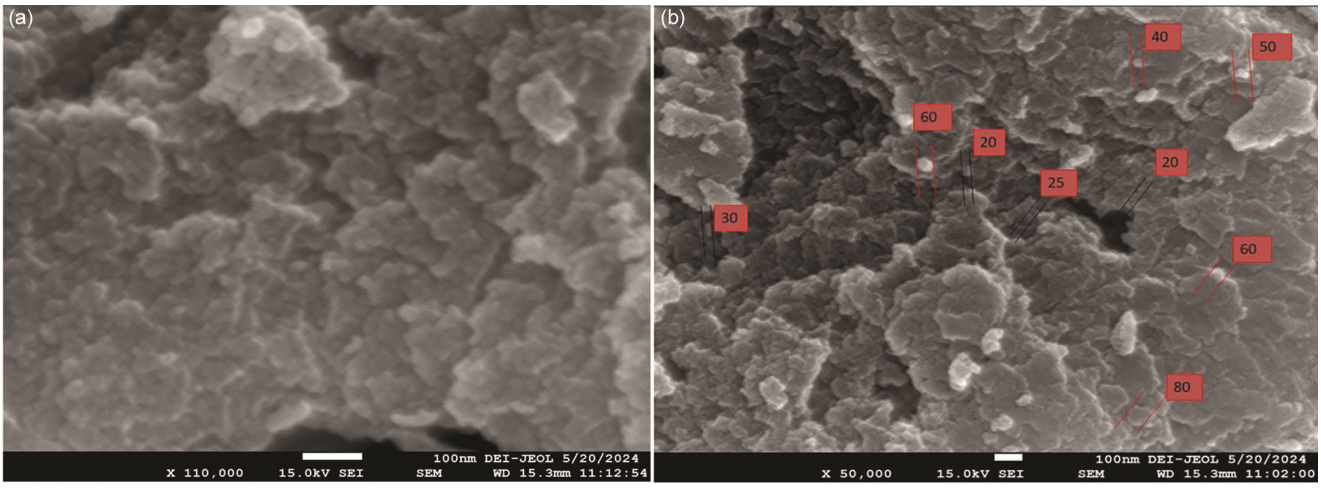

Fig. 3a-b — SEM image with ×1,10,000 magnification; (b) - SEM image with ×50,000 magnification

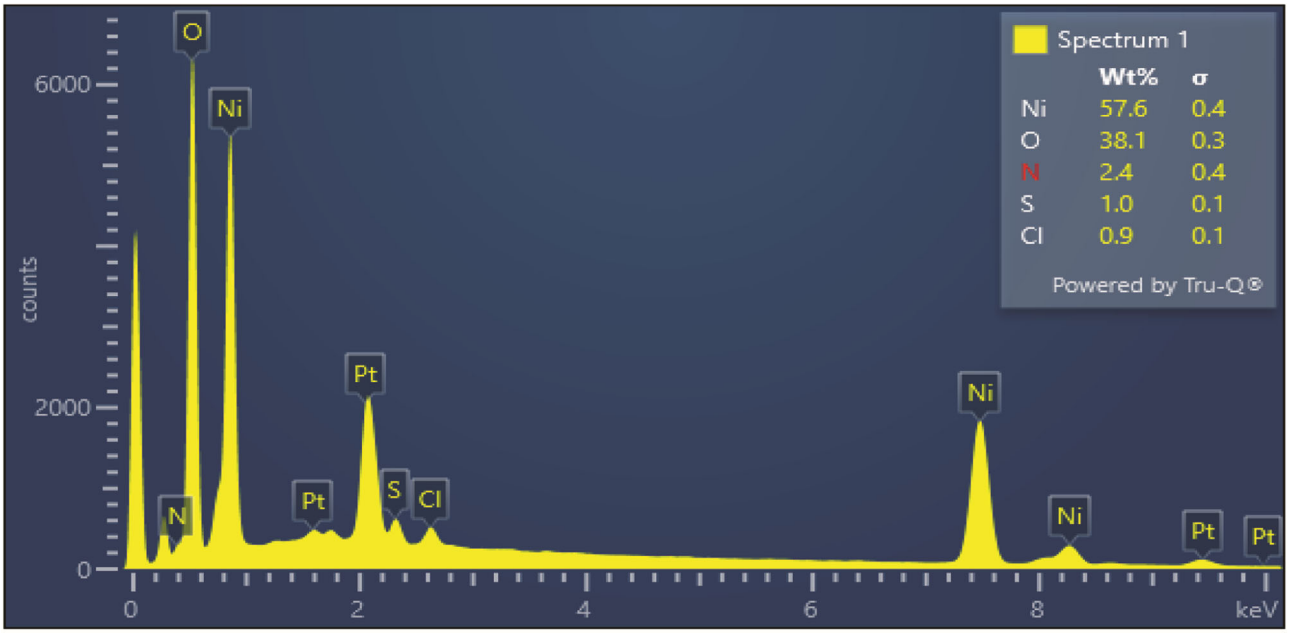

Fig. 4 — EDS analysis results of Ni-NPs

suggest it was excluded from quantitative analysis (possibly due to being a known coating or reference material). The table inset on the top right provides the weight percentages (Wt%) and their associated standard deviations (σ) for the quantified elements. Nickel and oxygen dominate, indicating that the material is likely a nickel oxide-based compound or alloy. The presence of nitrogen, sulfur, and chlorine in small amounts could arise from surface adsorption, environmental exposure, or synthesis residues.

This EDS spectrum suggests that the sample is predominantly composed of nickel and oxygen, possibly forming nickel oxide or a similar compound. The strong presence of oxygen supports this hypothesis. The trace elements (N, S, Cl) may influence surface chemistry or catalytic behaviour if the material is intended for such applications. Platinum peaks are prominent, but their absence in the quantification suggests it may be a coating material used to improve conductivity during SEM imaging rather than an inherent component of the sample.

Overall, this analysis provides vital insight into the chemical makeup of the sample, confirming its nickel-rich nature and hinting at potential surface modifications or contaminants. It is especially relevant in fields like materials science, catalysis, or battery research, where such compositions are common.

Photocatalytic activity of Synthesized Ni-NPs

Fig. 5 shows a set of UV-Vis absorbance spectra for two different dyes—Methylene Blue (MB) and Methyl Orange (MO)—under two different conditions: UV light irradiation and dark conditions, over various time intervals. Fig. 5(a-d) represents the photocatalytic results of the MB and MO.

These plots are commonly used to study the photocatalytic degradation behaviour of organic dyes in the presence of a catalyst and under specific environmental conditions.

For Methylene Blue under UV Light (MB UV), the absorbance spectrum shows a progressive decrease in peak intensity over time, especially around 660 nm, the characteristic peak of Methylene Blue. The decline in absorbance with time (from initial to 120 min) indicates the photocatalytic degradation of MB under UV light. The effectiveness of degradation is significant, as the peak intensity reduces considerably, reflecting the breakdown of dye molecules.

For Methylene Blue in Dark (MB Dark), this graph shows minimal change in absorbance over 120 minutes, suggesting negligible degradation of MB without UV exposure. This supports the idea that light is essential to activate the photocatalyst and initiate the degradation process. The constancy of the peak at ~660 nm over time confirms stability in the dark environment.

For Methyl Orange under UV Light (MO UV), the primary absorbance peak is observed at around 460 nm, which is characteristic of Methyl Orange. Like MB, the absorbance decreases progressively with time under UV irradiation, indicating successful

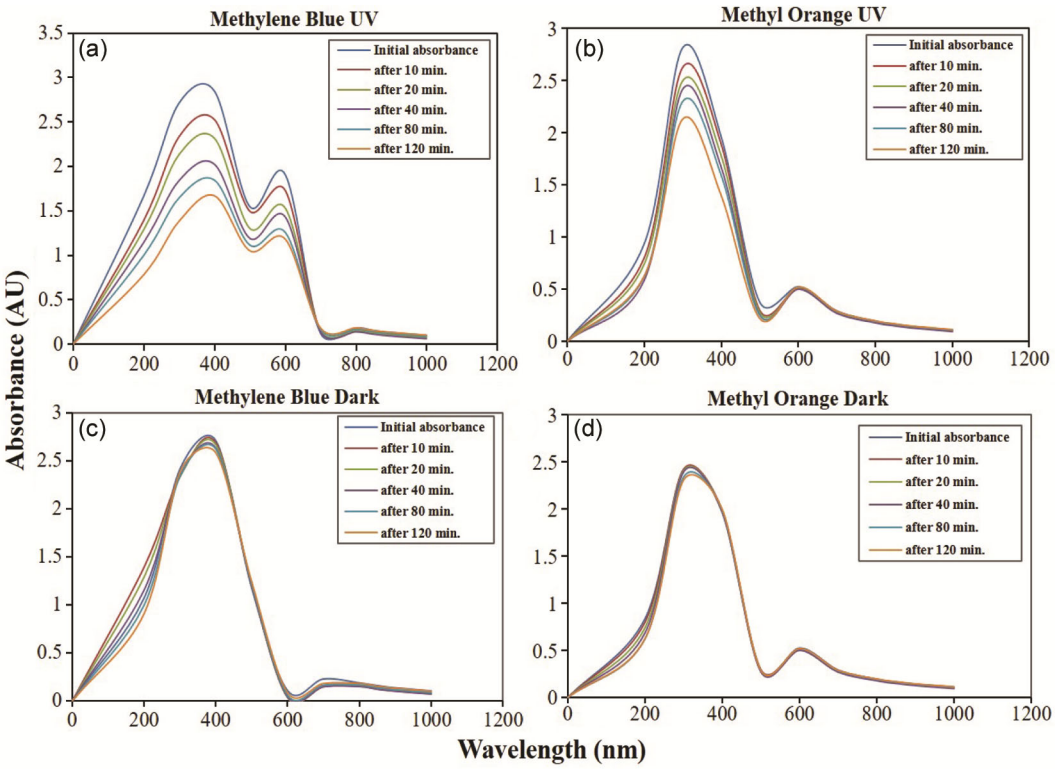

Fig. 5 — Photo-catalytic degradation of organic dyes under UV-light and dark conditions

photocatalytic breakdown of MO. The degradation is slower compared to MB, but still clearly visible over the 120-minute duration.

For Methyl Orange in Dark (MO Dark), there is minimal reduction in peak intensity over time, showing that MO is stable in the dark and no significant degradation occurs. This again confirms the UV-dependent activity of the photocatalyst. The results indicate that both Methylene Blue and Methyl Orange degrade significantly under UV light, but remain mostly unaffected in the dark. This strongly supports the presence and action of a UV-activated photocatalyst (likely the sample characterized in your earlier EDX image, possibly a NiO or Ni-based catalyst). The more rapid degradation of MB compared to MO may be due to differences in molecular structure, interaction with the catalyst, or light absorption efficiency.

This figure demonstrates the photocatalytic efficiency of the catalyst material in breaking down organic dye pollutants under UV light. The minimal degradation in dark conditions confirms the light-dependent mechanism, which is critical for validating photocatalytic applications in wastewater treatment or environmental remediation.

For the decolouration of organic dye, 100 mL of 20 ppm organic dye solution was prepared with the help of deionized water. To this solution, 0.1 mg of microwave-assisted green synthesized Ni-NPs was added and stirred well. The mechanism of organic dye degradation is described below. When a mixture of organic dye and synthesized nanoparticles is contacted with direct sunlight or UV sources, the following reaction takes place in the formation of active hydroxide and active oxygen species[25] (Din *et al.*, 2020).

$$NiO\text{-}NPs + h\upsilon \rightarrow h^{+}_{VB} + e^{-}_{CB}$$
$$O_2 + e^{-}_{CB} \rightarrow O_2^{-\bullet}$$
$$OH^{-} + h^{+}_{VB} \rightarrow OH^{\bullet}$$
$$Dye + OH^{\bullet} \rightarrow Degradable\ product$$
$$Dye + O_2^{-\bullet} \rightarrow Degradable\ product$$

The percentage of degradation of the dye was calculated by using the following equation,

$$Percentage\ degradation = C_o - C_t / C_o \times 100$$

C_o = initial concentration of organic dye

C_t = concentration of organic dye after t time

The percentage degradation of methylene blue and methyl orange was 41.34% and 28.9%, respectively. These results show that the decomposition was initiated effectively by the synthesized Ni-NPs, but due to the low concentration of catalyst, the percentage of decomposition was observed to be low,

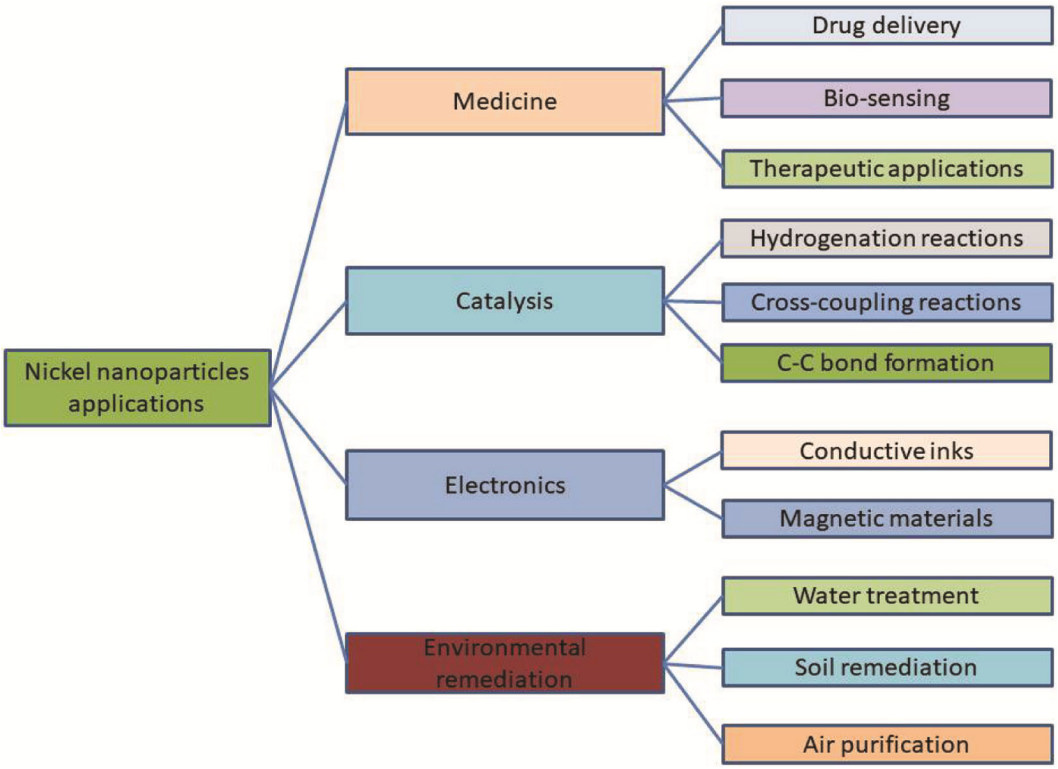

Fig. 6 — Applications of nickel nanoparticles

and the reaction was not completed after 120 minutes of reaction ignition.

Using a UV–Visible spectrophotometer (Systonics double beam spectrophotometer 2203), the optical and absorbance characteristics were found. A prominent absorption peak of 365 nm was visible in the UV–Vis spectrum of the nickel NP solution (Fig. 2). This peak developed as a result of surface Plasmon resonance occurring on the nickel NPs. Our results are supported by earlier reports, which show that a band of Ni-NPs is present at about 300 nm[24-26]. Nickel nanoparticles made from *T. cordifolia* stem extract show a spherical morphology and a particle size range of 40 to 80 nm at 10k and 50K time magnification in the SEM image (Fig. 3a and 3b). Energy dispersive spectroscopy (EDS) elemental analysis was performed (Fig. 4), revealing the weight percentages of Cl, O, Ni, and S to be 0.9%, 38.1%, 57.6%, and 1.0%, respectively. Ni's appearance confirmed the formation of nickel-based particles, and O's presence indicated the formation of nickel particles as a result of air and water reacting with the nickel NPs that have been formed[27]. These nanoparticles' high percentage composition of carbon and oxygen indicated that they are capped with organic groups of C–O functional groups, such as flavonoids and polyphenol compounds.

Applications of Microwave-Assisted Green Synthesized Ni-NPs

Ni-NPs are significantly used in various applications across the domains of medicine, catalysis, electronics, and environmental remediation, owing to their distinctive characteristics, including small size, wide surface area to volume ratio, and reactivity at the surface[24]. Hence, their applications are observed by the earlier workers as shown in Fig. 6. They can address diverse challenges in these sectors, positioning them as promising materials for driving future technological advancements[1].

Conclusions

Microwave-assisted green synthesis represents a promising approach for the sustainable production of nanoparticles with a reduced environmental impact. By utilizing eco-friendly precursors, microwave irradiation, and principles of green chemistry, this method provides a viable pathway toward green nanotechnology. Using this technique, we synthesized nickel nanoparticles with sizes ranging from 40 to 80 nm, with an average size of 30 nm, from a nickel nitrate hexahydrate salt solution and *T. cordifolia* stem extract. UV analysis confirmed the formation of the nanoparticles, while scanning electron microscopy

(SEM) provided insights into their size distribution. Additionally, energy-dispersive X-ray spectroscopy (EDS) graphs verified their composition and purity. The nickel nanoparticles (Ni-NPs) resulted in a 41.34% degradation of methylene blue and a 28.9% degradation of methyl orange. However, the degradation was incomplete, which can be attributed to low catalyst concentration and an incomplete reaction. Ongoing research is essential to fully unlock the potential of microwave-assisted green synthesis and its applications across various sectors.

Credit authorship contribution statement

Vishant Varma: Conceptualization, Investigation, Formal Analysis, Writing- Original Draft, Editing and Visualization. Sanjay Kumar Upadhyay: Supervision, Project Administration. Devbrat Pundhir: Supervision, Project Administration, Writing- Review and Editing.

Acknowledgments

The authors are thankful to the Council of Science and Technology, Lucknow, U.P., for the financial support in the form of a major research project (Sanction Order No CST/CHEM/D-1432 and Project Id: 2214).

References

1 Haider A, Muhammad I, Ali S, Haider J, Muhammad I, Hamid M, Iram S, Ali M M, Khan J A & Muhammad I, *Nano Res Lett*, 15 (2020) 1.
2 Patil S P, Chaudhari R Y & Nemade M S, *Talanta Open*, 5 (2022) 100083.
3 Dhas S D, Maldar P S, Patil M D, Nagare A B, Waikar M R, Sonkawade R G & Mohalkar A V, *Vacuum*, 181 (2020) 109646.
4 Olajire A A & Mohammed A A, *Adv Power Tech*, 31 (2019) 211
5 Hussain S, Muazzam A, Mahmood A, Muhammad A, Mustafa Z, Shahzad M, Ali J, Muhammad I, Muhammad S & Muhammad I, *J Taibah University science*, 17 (2023) 2170162.
6 Hafeez M, Ruzma S, Bilal A, Muhammad N A, Zain U A, Haq S, Salah U D, Zeb M & Khan M A, *S Afr J Chem* 75 (2021) 168
7 Barzinjy A A, Hamad S M, Aydın S, Ahmed M H & Hussian F H S, *J Mater Sci: Mater Elec*, 31 (2020) 11303.
8 Gunasekaran S S, Gopalakrishnan A, Bose S & Badhulika S, *J Energy Stor*, 37 (2021) 102412.
9 Prakash M V D, Sampath S, Amudha K, Ahmed N, Lopes B S, Durga B & Saravanan M, *Mat Tech*, 38 (2023) 2247908.
10 Rose A L, Vidhya S, Priya F J & Thattil P P, *Ijcrgg* 10 (2017) 377.
11 Chakraborty N, Banerjee J, Chakraborty P, Banerjee A, Chanda S, Ray K, Acharya K & Sarkar J, *Green Chem Lett Rev*, 15 (2022) 187.
12 Eluri R & Paul B, *Mat Lett*, 76 (2012) 36.
13 Ravichandran S, Sengodan P & Radhakrishnan J, *Cera Int*, 49 (2022) 12408.
14 Karthik K, Shashank M, Revathi V & Tatarchuk T, *Mol Cryst Liq Cryst*, 673 (2018) 70.
15 Kalwar N H, Soomro S R A, Sherazi S T H, Hallam K R & Khaskheli A R, *Int J Met*, 9 (2014) 1.
16 Khairnar S D & Shrivastava V S, *J Taibah Univ Sci*, 13 (2019) 1108.
17 Tsuji M, Hashimoto M, Nishizawa Y, Kubokawa M & Tsuji T, *Chem Eur J*, 11 (2005) 440.
18 Raj R A, Mohamad S A & Devanesan S, *Materials*, 10 (2017) 460
19 Mondal A, Mukherjee D & Mukherjee D K, *Int J Nano Tech*, 15 (2018) 736.
20 Khaskheli A R, Naz S, Soomro R A, Ozul F, Aljabour A, Kalwar N H, Abdul Mahesar W, Patir I H & Ersoz M, *Adv Mater Lett*, 7 (2016) 616.
21 Khalugarova K, Yuliya S, Moshnikov V, Alexey K & Kondratev V, *JBRES*, 4 (2023) 1136.
22 Soruma G ,F Guta G M & Ahmed A Y, *ACS Omega*, 7 (2022) 44720.
23 Habtemariam A B & Mohammed O, *Mat Int*, 2 (2020) 0205
24 Huang Y, Zhu C, Xie R & Ming N, *J Exp Nanosci,* 16 (2021) 368.
25 Din M I, Tariq M, Hussain Z & Khalid R, *Inorg Nano-Met Chem*, 50 (2020) 1.
26 Ahmed W & Rawat A, *Nat Env Poll Tech*, 22 (2023) 1353
27 Selvanathan V, Shahinuzzaman M, Selvanathan S, Sarkar D K, Algethami N, Alkhammash H I, Hannan F A, Zainuddin Z, Mohammod A, Abdullah H & Muhammad A, *Catalysts*, 11 (2011) 1523.